5026 *Biochemistry* **2009,** *48,* 5026–5033
DOI: 10.1021/bi900187s

BIOCHEMISTRY
including biophysical chemistry & molecular biology
Article

Humanin Structural Versatility and Interaction with Model Cerebral Cortex Membranes†

Sara Pistolesi,‡ Lara Rossini,§,∥ Elisa Ferro,§ Riccardo Basosi,‡ Lorenza Trabalzini,§ and Rebecca Pogni*,‡

‡*Department of Chemistry, University of Siena, Via A. De Gasperi, 53100 Siena, Italy, and*
§*Department of Molecular Biology, University of Siena, Via Fiorentina 1, 53100 Siena, Italy*
∥*Present address: Siena Biotech S.p.A., Strada del Petriccio Belriguardo 35, 53100 Siena, Italy*

Received February 5, 2009; Revised Manuscript Received April 9, 2009

ABSTRACT: Humanin (HN) is a recently identified neuroprotective peptide able to inhibit neurotoxicity induced by various insults which can be related to Alzheimer disease (AD) as well as to cell death induced by other stimuli. Previous CD and NMR studies demonstrated that HN adopts an unordered conformation in water, a α-helix conformation in 30% TFE, and a β-sheet structure in PBS. Furthermore, other studies clearly indicated HN as a secreted peptide, able to prevent neuronal cell death caused by amyloid β (Aβ) derivatives. Although Aβ was found to interact with neuronal membranes, currently there is not experimental evidence unveiling HN interaction with membranes. In this paper a spin labeling technique coupled with electron paramagnetic resonance (EPR) and circular dichroism (CD) has been used to study the structure and dynamics of HN in solution and for the first time in the presence of model cerebral cortex membranes (CCM). We have demonstrated that HN has a great tendency to aggregate even at low concentrations in water solutions at different ionic strengths and monomerizes in the TFE apolar environment. We also showed that HN slightly perturbs model CCM at the surface assuming a clear β-sheet conformation. In addition, HN increases the fluidity of the bilayer core without penetrating into the membrane.

Humanin (HN)[1] is a neuroprotective peptide of 24 amino acids able to antagonize neurotoxicity in neuronal cells and primary cultured neurons elicited by various Alzheimer's disease (AD) relevant insults, including AD-linked mutant genes and amyloid β (Aβ) peptide derivatives (*1*, *2*). It was suggested that HN is secreted from the cells (*2*) and may exert its neuroprotective activity through interactions with secreted factors or putative cell-surface receptors linked to tyrosine kinases (*3*−*6*). It has been demonstrated that HN is able to interact with the 40 aa form of Aβ ($A\beta_{40}$) and to affect Aβ aggregation dynamics and morphological features (*7*). In 2004, Ying et al., investigating the neuroprotective activity of secreted HN, demonstrated that the G-protein-coupled receptor FPRL1 shares both the 42 aa form of Aβ ($A\beta_{42}$) and HN, and it was suggested that HN may exert its neuroprotective effects by competitively inhibiting the access of Aβ to FPRL1 (*8*). Therefore, HN could protect neurons by exerting different functions, expected for its potential of binding different molecules on cell membranes (*7*).

The amphiphilic 40 and 42 residue peptides, $A\beta_{40}$ and $A\beta_{42}$, have been identified as the major components of senile plaques in patients with AD. They originate by proteolytic processing of a much larger amyloid precursor protein (APP) anchored in the brain membrane. The membrane release of Aβ peptides following this enzyme cleavage and their accumulation at the membrane surface is thought to be one of the first steps of membrane-associated Aβ fibrillogenesis and neurotoxicity (*9*). Despite their different aggregation properties and role in disease, the two peptides homogeneously co-mix in amyloid fibrils, suggesting that they possess the same structural architecture (*10*). Although a number of putative surface receptors for Aβ peptides have been described in the literature (*11*), a direct interaction with membrane components is thought to be a seed for the formation of toxic amyloid fibers (*9*, *12*−*14*). A conformational transition of peptides is necessary for fibril formation (*9*, *15*).

Despite the HN capability to inhibit toxicity induced by AD-related insults in neurons, it was demonstrated that HN exerts a protective effect also on nonneuronal cells when they are exposed to AD-related cytotoxicity (*16*). Further investigations showed that HN possesses a wide spectrum of action (*17*). Moreover, it has been demonstrated that HN is able to interact

†The work was supported by the Fondazione Monte dei Paschi di Siena (Project Number 29970, 2007, to L.T.) and University of Siena (PAR 2006 to R.P.).

*To whom correspondence should be addressed. Fax: (+39) 0577 234239. Phone: (+39) 0577 234258 E-mail: pogni@unisi.it.

[1]Abbreviations: Aβ, amyloid β; AD, Alzheimer's disease; AMP, antimicrobial peptides; APP, amyloid precursor protein; CCM, cerebral cortex membrane; CD, circular dichroism; Cer, galactocerebroside; Ch, cholesterol; EPR, electron paramagnetic resonance; FPRL1, formylpeptide receptor-like 1; GM1, monosialoganglioside GM1; HN, humanin; HNG, S14G humanin mutant; HNSL, spin-labeled humanin; LUV, large unilamellar vescicles; MOPS, 4-morpholinepropanesulfonic acid; MTSSL, 1-oxy-2,2,5,5-tetramethylpyrroline-3-methyl methanethiosulfonate; NMR, nuclear magnetic resonance; *n*-PCSL, 1-(*n*-doxylpalmitoyl)-2-stearoylphosphatidylcholine; PBS, phosphate-buffered saline; PC, 1-palmitoyl-2-oleoylphosphatidylcholine; PE, 1-palmitoyl-2-oleoylphosphatidylethanolamine; PS, 1-palmitoyl-2-oleoylphosphatidylserine; SDSL, site-directed spin labeling; SM, sphingomyelin; TFE, trifluoroethanol.

 Published on Web 04/20/2009

with intracellular proteins such as Trim11 (*18*) and the three proapoptotic factors Bax (*19*), Bid (*20*) and BimEL (*21*), thus suggesting that intracellular mechanisms are also possible (*16*).

While extensive studies have been carried out on the biological function of HN, only a few structural studies were performed. These were done in acidic conditions and at concentrations far away from the effective levels. Structure−function analyses suggested that HN acts as a multimer and that specific mutations disturbing self-dimerization affect the neuroprotective activity (*17*). CD experiments revealed that both HN and its analogue HNG (S14G mutant), 1000-fold more active, are disordered in acidic water solution independently from concentration while adopt a β-sheet conformation in PBS at neutral pH (*22*, *23*). On the other hand, one of the most active HN derivatives, AGA (C8R)HNG17 (1000-fold more active than HNG), was reported to fold in β-sheet also in water (*24*). This evidence suggested the tendency of the peptide to hydrophobically interact with other structures as well as with itself. NMR studies performed in 30% TFE at pH ~3 and millimolar concentration showed that both HN and HNG undergo to conformational transition assuming an α-helix secondary structure (*25*, *26*).

Here a spin labeling technique coupled to EPR spectroscopy and CD is used to study the solution structural properties of HN at physiological pH and micromolar concentrations.

The spin labeling technique has been successfully used to study structural features and the dynamics of soluble as well as membrane proteins (*10*, *27*−*38*). These studies gave further help in understanding the mechanism through which antimicrobial peptides (AMP) kill bacteria exploiting the nature of peptide/membrane interaction (*31*−*34*). Recent studies indicate that this strategy is also well suited for studying amyloid fibrils (*10*, *35*−*37*).

Compared to other spectroscopic techniques, EPR takes advantage from its sensitivity, thus permitting the study of systems even in the low micromolar range.

The main purpose of this paper is the elucidation of the influence of HN on cerebral cortex membranes (CCM) in order to help the understanding of the mechanism of action of this neuroprotective peptide. Additionally, we also wanted to investigate HN structural properties in different conditions by operating at physiological pH and micromolar HN concentrations, thus getting closer to HN effective doses (1−10 μM) (*17*).

EXPERIMENTAL PROCEDURES

Materials. HN was purchased from VWR International SRL (Milano, Italy). MOPS (4-morpholinepropanesulfonic acid) and trifluoroethanol (TFE) were from Sigma-Aldrich (St. Louis, MO). The methanethiosulfonate spin label, MTSSL (1-oxy-2,2,5,5-tetramethylpyrroline-3-methyl methanethiosulfonate) was obtained from Toronto Research Chemicals (North York, Ontario, Canada). 1-Palmitoyl-2-oleoylphosphatidylcholine (PC), 1-palmitoyl-2-oleoylphosphatidylethanolamine (PE), 1-palmitoyl-2-oleoylphosphatidylserine (PS), galactocerebroside (Cer), sphingomyelin (SM), cholesterol (Ch), monosialoganglioside GM1 (GM1) and *n*-PCSL (1-(*n*-doxylpalmitoyl)-2-stearoylphosphatidylcholine; n = 5, 7, 12) spin labels were obtained from Avanti Polar Lipids (Alabaster, AL).

Peptide Spin Labeling and Purification. Peptides used in this work were HN (MAPRGFSCLLLLTSEIDLPVKRRA) and its spin-labeled derivative (HNSL). The native peptide was solubilized in 50 mM MOPS, pH 6.8, to get a 2 mg/mL solution (0.75 mM), aliquoted for subsequent use, and stored at 253 K.

Table 1: Composition of Real and Model Cerebral Cortex Membranes

	cerebral cortex lipid (w/w %)	CCM−lipid (mol %)
PC	13.9	14
PS	8.0	7
PE	23.9	24
SM	8.0	4
Ch	13.3	26
Cer	14.3	15
GM1	8.75	4
plasmalogen	9.94	

For spin labeling, native HN containing a native cysteine in position 8 was incubated overnight at 277 K under agitation with a 5-fold molar excess of MTSSL spin label. To remove unreacted spin label, peptide was purified by reverse-phase high-performance liquid chromatography on a 10 μm, 4.6 mm × 250 mm C12 column (Vydac, Hesperia, CA) using a linear gradient of 10−80% acetonitrile/0.1% trifluoroacetic acid (TFA) in water/0.1% TFA over 60 min. The spin-labeled peptide (HNSL) was then lyophilized, solubilized in 50 mM MOPS, pH 6.8, at a final concentration of 1 mM, aliquoted, and stored at 253 K until use. The stability of the spin label attached to the peptide was periodically checked by HPLC.

Model Cerebral Cortex Membrane (CCM) Preparation. Model CCM were prepared in agreement with the composition of cerebral cortex membrane lipids as already described and reported in Table 1 (*9*). Lipids in the desired molar ratio were dried down from chloroform stock solutions under a stream of nitrogen gas and then dried overnight under vacuum. The resulting lipid film was hydrated by the addition of 50 mM MOPS, pH 6.8, to give a concentration of 50 mM phospholipid. Large unilamellar vesicles (LUVs) of model cerebral cortex membranes were prepared by freeze−thawing this lipid suspension five times, followed by extrusion through 200 nm polycarbonate membrane filters using a miniextruder syringe device (Avanti Polar Lipids). Final lipid concentration was measured by the method of Stewart (*39*). LUVs containing 1 mol % of 5-, 7-, or 12-PCSL were prepared as described above. HN stock solution was added to membranes in an appropriate ratio and incubated for 30 min at room temperature.

CD Spectropolarimetry. CD spectra of HN in the range 250−190 nm were recorded on a Jasco J715 spectropolarimeter using 1 mm quartz cells, 1 nm bandwidth, 0.2 nm resolution, 1 s response, and an average of 10 scans for each spectrum. The CD spectrum of the spin-labeled HN was recorded and compared with that of unlabeled peptide, and the two spectra were identical. CD spectra of HN with CCM were obtained, subtracting the blank composed by the same amounts of CCM.

EPR Spectroscopy. X-band EPR measurements were performed on an Elexsys E-500 spectrometer (Bruker, Germany). Fifteen microliters of HNSL samples was loaded in quartz capillaries (0.84 mm o.d. × 0.6 mm i.d.) sealed at one end. All spectra were acquired using a 10 dB attenuation. Scan width was 100 G, and the acquisition parameters were chosen to improve the signal-to-noise ratio without generating line broadening.

The apparent correlation time τ_c was determined according to (*29*)

$$\tau_c = (0.65 \times 10^{-9})\Delta H_0 \equiv [(A_0/A_{-1})^{1/2} - 1] \Downarrow$$

where ΔH_0 is the peak-to-peak width of the center line in gauss, A_0 is the amplitude of the center line, and A_{-1} is the amplitude of the high-field line.

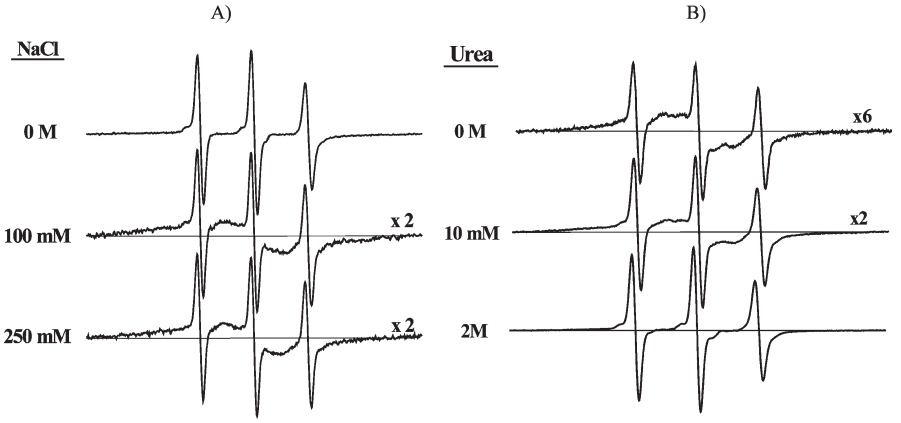

FIGURE 1: EPR spectra of HN in the presence of different concentrations of NaCl (A) and urea (B). The solutions contained 50 mM MOPS, pH 6.8, and 50 μM HNSL.

All the measurements were repeated three times from independent samples to calculate standard errors.

RESULTS

HN Behavior in Solution. EPR spectra of HNSL in aqueous solution at different ionic strengths are shown in Figure 1A. The three narrow lines present in the spectra indicate the presence of a population of peptides in which the spin label is undergoing rapid isotropic motion with a correlation time of about 0.2 ns, indicative of peptide in a random coil conformation as confirmed by the CD spectrum (see Figure 2, trace A). Addition of NaCl results in the appearance of an extensively exchange-broadened line underlying the EPR spectrum, as indicated by the asymmetric baseline and decreased signal amplitude (Figure 1A). This single broadened line might arise from pronounced spin−spin interaction due to peptide self-association that brings spin-labeled sites into close proximity. Moreover, the nearly identical 100 and 250 mM NaCl spectra are consistent with a stable equilibrium between random coil peptide and oligomers or aggregates (three sharp lines and a single broadened line, respectively). Salts are known to stabilize aggregates if they are formed by hydrophobic forces or electrostatic repulsion, while the opposite effect is obtained if salt bridges are involved. We found that 100 mM NaCl concentration is enough to induce the formation of a stable aggregate which no longer dissociates at higher ionic strengths. These findings rule out the possibility of a salt bridge stabilized aggregate and support hydrophobic forces and/or electrostatic repulsion factors as the basis for aggregation. The effect of urea on aggregate stability has been also examined (Figure 1B). Urea is known to increase nonpolar side-chain solubility while maintaining the hydrogen-bonding capability of aqueous solvents. Addition of 10 mM urea leads to a destabilization of the aggregate where only a small percentage of the characteristic single broadened line due to aggregation is maintained and spectral amplitude is increased. This is also consistent with the peptide monomerization in the presence of urea confirming the hydrophobic nature of the aggregate.

In Figure 2 CD spectra of 50 μM HN in different conditions are shown. In aqueous solution (Figure 2, trace A), the CD spectrum shows a strong negative peak at 197 nm, indicative of a disordered peptide. On addition of 30% TFE (Figure 2, trace B), the negative band is shifted to 206 nm, a second negative band shows up at 222 nm, while a positive peak is present at 190 nm. These changes are indicative of a conformational transition

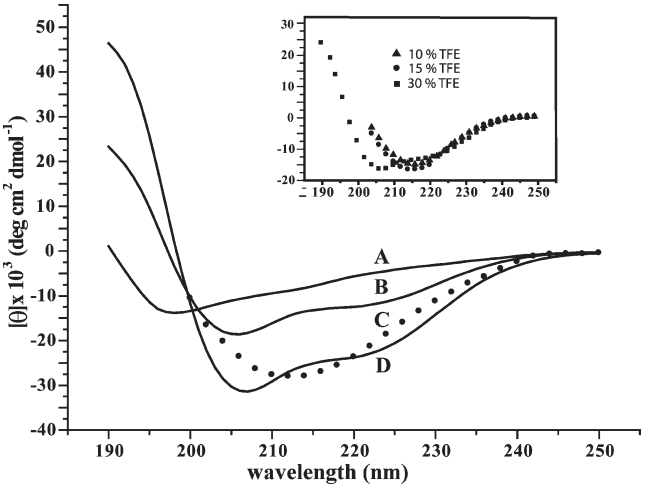

FIGURE 2: CD spectra of 50 μM HN in (A) 50 mM MOPS, pH 6.8, (B) 30% TFE, (C) 250 mM NaCl (dotted line), and (D) 98% TFE. Spectrum C was recorded above 200 nm because of technical problems with salts. Inset: CD spectra of 50 μM HN in 10% TFE (triangles) and 15% TFE (circles). The 30% TFE CD spectrum (squares) is also shown for comparison. The pH was 6.8.

between unordered and helical conformation. CD spectra of HN with 250 mM NaCl (Figure 2, trace C) show a negative band shifted to 212 nm and resemble a β-sheet conformation which is probably in equilibrium with a random coil structure, as was previously found in PBS (high ionic strength medium) for the mutated peptides HNG (S14G mutation) (*22*) and AGA(C8R) HNG17 (*24*). In fact, the negative peak is located at 212 nm, which is comprised between the typical negative peaks for unordered and β-sheet structures, 196 and 216 nm, respectively (see also Figure 9 below). This result is consistent with the two-component EPR spectra reported above for HNSL in 250 mM NaCl (Figure 1).

It is worth noting that CD spectra of 50 μM HN in 10% and 15% TFE (Figure 2, inset) are very similar in line shape to that of HN in 250 mM NaCl, although the negative band is shifted exactly at 216 nm. Then, below 30% TFE, HN adopts a β-sheet conformation and the isodichroic point at about 210 nm indicates a simple two-state equilibrium between α-helix and β-sheet secondary structures.

The further helical content increase observed upon addition of 98% TFE (Figure 2, trace D) in respect to 30% TFE may be explained as a more pronounced helicity of the peptide or oligomerization.

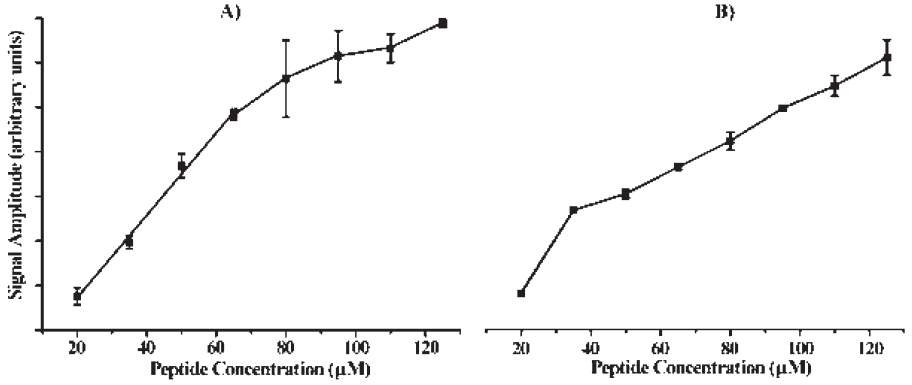

FIGURE 3: Signal amplitudes of the $m_I(0)$ resonance line of HN spectra in the function of peptide concentration. Panel A refers to HNSL in 50 mM MOPS, pH 6.8, and panel B is relative to HNSL in 100 mM NaCl solution. Standard errors were calculated from three independent measurements.

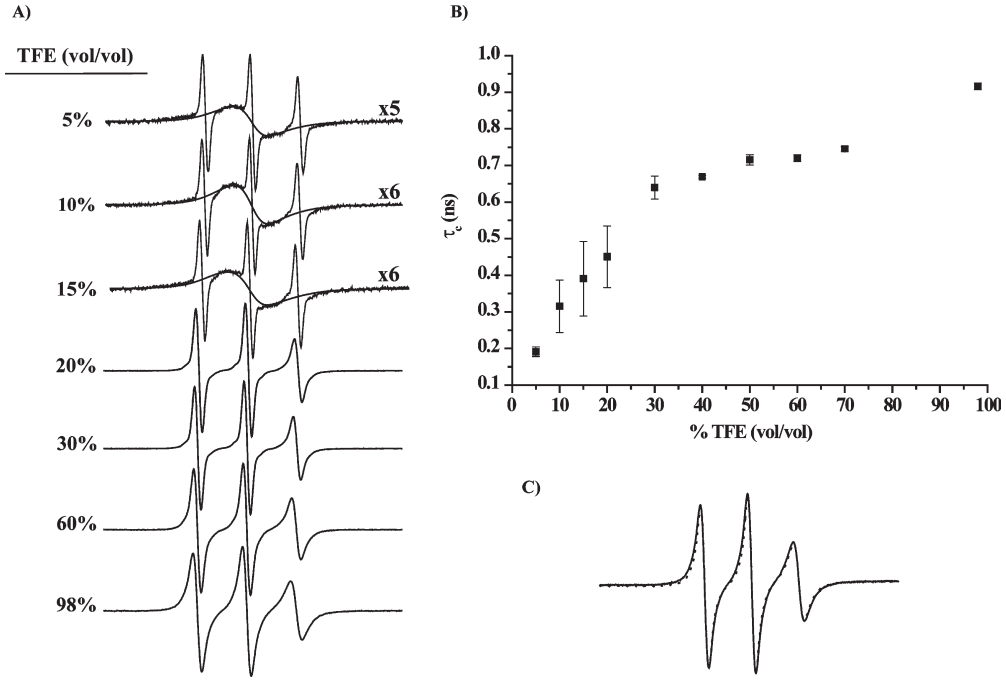

FIGURE 4: (A) EPR spectra of 50 μM HNSL with different concentrations of TFE. (B) Correlation times vs TFE percentages for 50 μM HNSL. Standard errors were calculated from three independent measurements. (C) EPR spectra of 50 μM HNSL in 98% TFE (straight line) and of 50 μM HNSL in 98% TFE plus 350 μM native HN (dotted line).

To investigate if aggregation occurs in an aqueous environment, EPR spectra in water solutions at different ionic strengths were recorded at increasing HNSL concentration (Figure 3). In the absence of NaCl (Figure 3A), the central line amplitude linearly increases until the critical concentration of 65 μM and raises only slightly at higher peptide concentrations. In the presence of 100 mM NaCl (Figure 3B), the critical concentration for aggregation decreases to 35 μM. Above this value, the $m_I(0)$ line amplitude linearly increases with increasing amounts of HNSL, indicating a constant contribution of spin−spin interaction to intensity (*31*). These results suggest that HN has the tendency to form aggregates and/or oligomers in aqueous solution, and at higher ionic strengths aggregation is even more pronounced. These data, in combination with the CD spectrum described above, indicate that β-sheet conformation found for HN in 250 mM NaCl (Figure 2, trace C) could be related to an aggregate.

Figure 4A shows EPR spectra of HNSL in the presence of increasing volumes of TFE. From 5% to 15% TFE a three sharp line component with a correlation time below 0.6 ns overlaps with very broad single line, suggesting an equilibrium between monomeric unfolded peptide and an exchange-broadened aggregate. Interestingly, CD spectra of HN in the presence of 10% and 15% TFE (see inset in Figure 2) showing a negative band at 216 nm are typical of a β-sheet structure. Then, the broadened line could be associated to β-sheet aggregated HN. In the 20−30% TFE range the spectra reflect the presence of a folded species with no evidence for aggregation.

Correlation time analysis upon TFE addition (Figure 4B) reveals two different slopes. Between 5% and 30% TFE, τ_c (of the monomeric species) rapidly increases (i.e., motion decreases). The increase of τ_c value probably reflects an increased folding of the monomer in the 5−30% TFE range. At 30% TFE, the τ_c value (about 0.65 ns) is consistent with the presence of a monomer in a folded α-helical conformation, as also indicated by the CD spectrum of HN (Figure 2, trace B). Also, diluting the spin-labeled HN with a 6-fold native peptide does not change the spectral shape (data not shown).

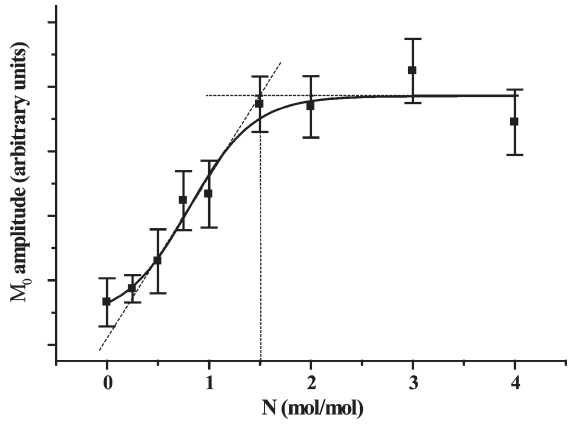

FIGURE 5: Dependence of the $m_I = 0$ resonance line amplitude on the molar ratio (N mol/mol) of native and labeled HN (HNSL) in the presence of 10% TFE. In each sample HNSL concentration was kept constant at 50 μM while the concentration of native HN was increased.

As the TFE concentration is increased from 30% to 98%, the EPR lines broaden and the calculated τ_c continues to increase, albeit at a lower rate than below 30% TFE (Figure 4B). The changes seen from 30% to 98% TFE may reflect an increasing percentage of a folded, apparently compact, species that is more α-helical than the species found at 30% TFE or the presence of an aggregate and/or oligomer. In Figure 4C the EPR spectrum of HNSL is overlapped with that of HNSL diluted with a 6-fold molar excess of native HN. No spectral changes are detected, thus excluding aggregation-dependent broadening. This is consistent only with an increased helicity of the peptide. In other words, the protein is rapidly exchanging between a more flexible (found at 30% TFE) and a more compact (found at 98% TFE) monomer conformation. This explanation is consistent with CD data. As noted above, the CD spectrum of HN in 98% TFE (Figure 2, trace D) represents a greater α-helical content as compared to 30% TFE.

To further validate the formation of an aggregated form below 30% TFE, the EPR signal amplitude was analyzed in the presence of different spin-labeled/native HN ratios. In fact, if the aggregate contains more than one spin-labeled monomer, the spin labels can interact by electron dipole−dipole interaction or by Heisenberg exchange, leading to a significant drop in signal amplitude. Thus, diluting the spin-labeled monomers in the aggregate with native HN should induce an increase in signal amplitude of three line spectra. Figure 5 shows the dependence of the $m_I(0)$ resonance line amplitude on the molar ratio between native and spin-labeled HN (N, mol/mol) in the presence of 10% TFE. Signal amplitude increases by adding increasing amounts of native HN up to a ratio of about 1:1.5 (HNSL:HN), while above $N = 1.5$ the central resonance line amplitude remains constant. More interestingly, signal amplitude increases until the molar ratio of 1:1.5, which corresponds to about one spin-labeled monomer and one native monomer, or in other words to a dimer or oligomers formed by dimers. These data confirm the presence of a very stable oligomer in which the spin labels are in close contact.

Motional restriction also plays a role in producing a broadening in the resonance lines. Diluting the spin labels in the putative aggregate, together with the elimination of spin−spin interaction, should allow observation of the motional behavior of the spin label in the aggregate. In Figure 6, HNSL spectra diluted with native peptide in the presence of 10% TFE are represented.

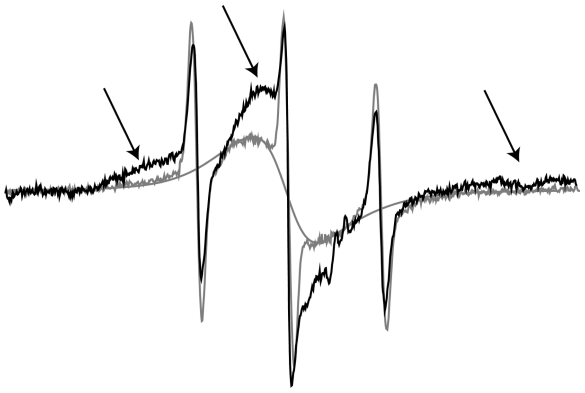

FIGURE 6: Comparison between 50 μM HNSL in 10% TFE alone (gray) and with a 6-fold molar excess of native HN (black). Samples contained 50 μM HNSL, 300 μM native HN, and 50 mM MOPS, pH 6.8. Scan width = 100 G.

Based on the data reported in Figure 4C, a 6-fold excess of native HN was chosen to ensure the elimination of any dipolar broadening contribution. We have previously shown that, in the range from 5% to 15% TFE, EPR spectra are characterized by an aggregate associated with the single broadened line and that the stoichiometry of the aggregate is that of a dimer. Here the single broadened line (see Figure 6, gray line) has virtually disappeared, leaving in its place an immobilized species (see Figure 6, black line) corresponding to the motionally restricted aggregate which is always in equilibrium with unfolded peptide (three sharp lines). As reported in Figure 4A, when the TFE concentration is further increased, the immobilized species continues to diminish, and at 30% TFE the peptide is completely monomeric.

Effect of HN on Model Cerebral Cortex Membranes (CCM). Phospholipid bilayers are structurally more compact on the surface and more fluid in the core due to different packing conditions. EPR spectra of CCM spin labeled in positions 5, 7, and 12 (see Figure 7) reflect this pattern. In going from the surface to the interior the major hyperfine splitting ($2A_{zz}$) becomes smaller, meaning that the rotational motion of the spin label increases from position 5 to position 12. It is worth noting that the line shape of the three spectra is typical of a single immobilized population of spins (only one component), although at different freedom degrees depending on the position in the alkyl chain. The presence of cholesterol in our model membranes leads to a higher degree of ordering also in the hydrophobic interior of the bilayers. This is the reason why even the 12-PCSL−CCM is characterized by an order parameter of about 0.65.

To assess the effects of HN binding on the lipid phase of the bilayer, we examined the motional parameters for spin-labeled CCM (Figure 8). For 5-PCSL, a plot of the motional parameter $2\Delta A_{zz}$ as a function of the peptide to lipid ratio suggests a slight decrease in motion (i.e., an increase in $2A_{zz}$) with increasing concentration of bound peptide. A similar trend is observed for 7-PCSL, although changes are smaller than for 5-PCSL. For 12-PCSL increasing concentrations of peptide lead to a small increase in rotational freedom (i.e., the hyperfine splitting $2A_{zz}$ decreases) as if the presence of HN induced a rising of the fluidity in the core of the bilayer while a higher density on the surface. These results indicate that perturbation of bilayer lipid motional dynamics upon accumulation of bound HN is observed across the entire length of the membrane with opposite effects on the surface and in the hydrophobic region, and even those effects are minimal. The stoichiometry of the interaction can be estimated by extrapolation of the increase in $2\Delta A_{zz}$, on initial tight binding,

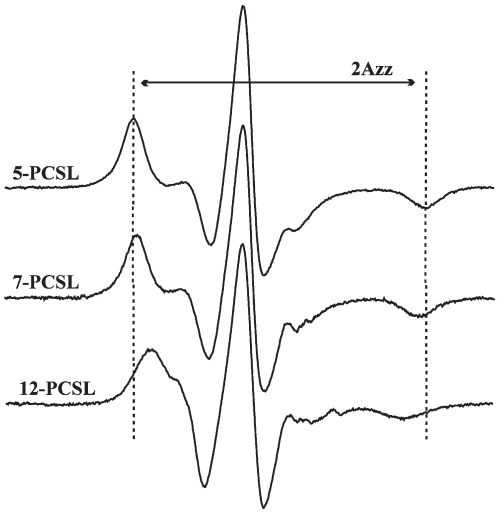

FIGURE 7: EPR spectra of 5-, 7-, and 12-PCSL in model CCM. The scan width is 100 G.

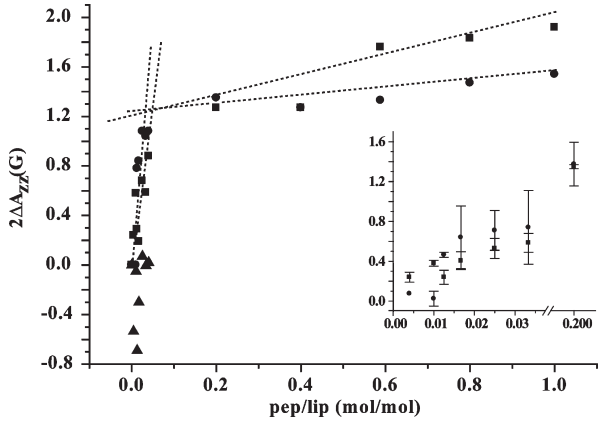

FIGURE 8: $2\Delta A_{zz}$ dependence in outer splitting of spin-labeled CCM on increasing HN/CCM molar ratio for 5-PCSL (circles), 7-PCSL (squares), and 12-PCSL (triangles). $2A_{zz}$ values for 5-, 7-, and 12-PCSL without peptide are 60, 58, and 52 G, respectively. The expansion of the 0.0−0.2 peptide/lipid molar ratio region with the corresponding standard errors has been reported in the inset.

to the saturation value of $2\Delta A_{zz}$. This yields a stoichiometry of about 1:25 peptide to lipid molar ratio.

Stated that HN presence on the model CCM does not significantly perturb the bilayer except only slightly the surface, we investigated also HN structural properties in the presence of CCM by CD (see Figure 9). In the presence of increasing amounts of CCM lipids, HN undergoes a conformational transition from random coil structure to a well-defined β-sheet arrangement characterized by a positive band at 196 nm and a negative band at 219 nm of comparable magnitude. While the line shape remains exactly the same, the amplitude of the CD spectra diminishes while going to increasing peptide to lipid ratios. This finding could be related to a change in HN structure upon addition of bigger amounts of CCM or to a change in the oligomerization state. Since no shape changes are observed, the secondary structure of HN bound to membranes is clearly conserved over all of the studied ratios. Thus, the amplitude decrease could to be due to the loss of the aggregation state.

DISCUSSION

In this study, the neuroprotective HN peptide has been thoroughly investigated in a variety of experimental conditions

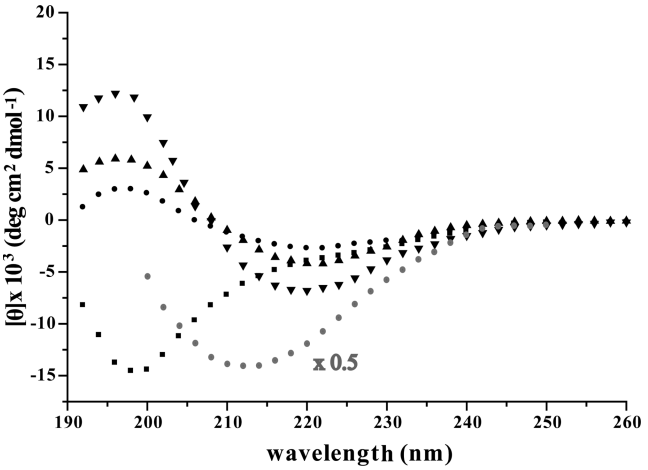

FIGURE 9: CD spectra of 50 μM HN in the presence of different molar ratios of CCM. HN in 50 mM MOPS, pH 6.8 (squares), 1:25 HN/CCM (circles), 1:50 HN/CCM (up triangles), and 1:100 HN/CCM (down triangles). The CD spectrum of 50 μM HN in 250 mM NaCl (gray) is reported for comparison.

showing its great variability in secondary structure and aggregation states.

Previous CD and NMR studies have shown that HN is monomeric and unfolded in water (*23*, *25*), in the apolar solvent TFE it adopts an α-helix conformation reaching its maximum helicity at 30% TFE (*25*), while it assumes a β-sheet structure in PBS at high HN concentrations (370 μM) (*23*). Interestingly, the ability of HN and its derivatives to assume a β-sheet conformation has been related to their neuroprotective activity (*24*). However, HN was found to adopt an α-helix secondary structure when associated to the hydrophobic pocket of the proapoptotic protein Bid (*40*).

We found that 50 μM HN in aqueous solution is in a random coil conformation and undergoes a conformational transition when 30% TFE is added. In addition to these findings the existence of an aggregated form of HN in TFE has been also demonstrated. The presence of an aggregate, represented by the single exchange-broadened line is evident in the concentration range of 5−15% (Figure 4A). This feature completely disappears when 30% TFE is added, thus suggesting that in an apolar environment HN is folded in a monomeric form, converging to achievements of previous CD studies performed in acidic solutions (*25*). The existence of an aggregated form of HN has been also demonstrated at high ionic strengths. The CD spectrum of HN with 250 mM NaCl revealed the secondary structure of this aggregate. Thus, we concluded that at high ionic strengths HN is in equilibrium between an unstructured and a β-sheet structured conformation.

Notably, in this study, HN interaction with model membranes has been investigated by using spin labeling EPR combined with CD measurements. All data were recorded at physiological pH and at HN micromolar concentrations, thus getting closer to the HN effective dose (1−10 μM) (*17*).

The EPR spectroscopy of spin-labeled lipids has proven to be a most useful means of studying protein−lipid interactions with peripheral as well as integral proteins in membranes. By coupling EPR with CD spectroscopy, we were able to monitor the variation in secondary structure of HN following its interaction with membranes.

Liposomes used in this work constitute a more complex system compared to model membranes commonly used for peptide−lipid

interaction studies (*27*−*29*, *32*−*34*). The lipid composition of our model membranes was very similar to CCM (*9*) except for the absence of plasmalogen due to its instability in our experimental conditions. However, it has been reported that levels of plasmalogen in AD CCM are reduced (*41*).

It has been suggested that HN may exert its neuroprotective function in extracellular environment through interactions with secreted factors or putative membrane receptors (*2*−*6*) or by competing with Aβ peptide in the binding to FPRL1 receptor (*8*). Furthermore, recent studies have shown that the interaction of Aβ and lipids plays an important role in the pathogenesis of AD. For instance, the fibrillogenic properties of Aβ are in part a consequence of the composition of the membrane in which it resides, its peptide sequence, and its mode of assembly (*42*). The presence of Ch and GM1 in neuronal membranes was shown to be crucial for fibrillogenesis and neurotoxicity (*9*, *43*, *44*). The negatively charged sialic acid of GM1 was stated to be the anchoring point of Aβ to the surface of the membrane that favors fibril formation. In the presence of GM1, Aβ is hypothesized to undergo a conformational transition from an α-helix to a β-structure leading to fibril formation (*9*).

By examining the motional parameters of the 5-PCSL and 7-PCSL lipids tested, the outer hyperfine splitting, $2A_{max}$, is greater for the HN-bound membranes than for the free lipid membranes, while for 12-PCSL a little decrease in $2A_{max}$ has been observed when HN is present. As the increase in $2A_{max}$ is related to a more ordered and decreased fluidity, and the opposite for decreasing values of $2A_{max}$, we observed that HN induces a motional decrease on the surface of CCM caused by superficial accumulation and at the same time causes a little increase in fluidity in the core region. The values of $2\Delta A_{zz}$ are less than 2 G for all of the peptide/lipid molar ratios examined and are in agreement with the values reported in the literature for other nonpenetrating peptides like α-synuclein (*45*), truncated α-synuclein (*46*), and others (*47*). Furthermore, HN binds to CCM assuming a β-sheet conformation structure, as is shown in Figure 9. This feature is also marked in the more potent derivative of HN, AGA-(C8R)HNG17, which assumes a β-sheet structure also in water solution (*24*). Notably, we found that the stoichiometry of HN−membrane lipid interaction is about 1:25. As in our model membranes GM1 is present as 4% mol, we may assume that HN and GM1 are present at 1:1 molar ratio. Based on that, a possible interaction of HN with GM1 might be hypothesized. Thus, HN can exert its neuroprotective activity interacting with the same molecular target of Aβ on the cell membranes. It has been also demonstrated that HN is able to interact with Aβ, preventing Aβ neurotoxic effects through morphological and functional alterations of the peptide (*7*). These different evidences indicate that HN could exert its neuroprotective function by binding different molecules on cell membranes.

In conclusion, HN may play a variety of different roles thank to its ability to change conformation. It is able to bind hydrophobic pockets of proteins as an α-helical monomer (*40*), but when located on liposomes mimicking the plasma membrane, it assumes a clear β-sheet secondary structure.

Our work is an additional confirmation of HN structural versatility and might contribute to clarify the multiple roles and mechanisms of HN neuroprotection.

REFERENCES

1. Hashimoto, Y., Niikura, T., Tajima, H., Yasukawa, T., Sudo, H., Ito, Y., Kita, Y., Kawasumi, M., Kouyama, K., Doyu, M., Sobue, G., Koide, T., Tsuji, S., Lang, J., Kurokawa, K., and Nishimoto, I. (2001) A rescue factor abolishing neuronal cell death by a wide spectrum of familial Alzheimer's disease genes and Aβ. *Proc. Natl. Acad. Sci. U.S.A. 98*, 6336–6341.
2. Hashimoto, Y., Ito, Y., Niikura, T., Shao, Z., Hata, M., Oyama, F., and Nishimoto, I. (2001) Mechanisms of neuroprotection by a novel rescue factor humanin from Swedish mutant amyloid precursor protein. *Biochem. Biophys. Res. Commun. 283*, 460–468.
3. Ikonen, M., Liu, B., Hashimoto, Y., Ma, L., Lee, K.-W-, Niikura, T., Nishimoto, I., and Cohen, P. (2003) Interaction between the Alzheimer's survival peptide humanin and insulin-like growth factor-binding protein 3 regulates cell survival and apoptosis. *Proc. Natl. Acad. Sci. U.S.A. 100*, 13042–13047.
4. Nishimoto, I., Matsuoka, M, and Niikura, T. (2004) Unravelling the role of humanin. *Trends Mol. Med. 10*, 102–105.
5. Harada, M., Habata, Y., Hosoya, M., Nishi, K., Fujii, R., Kobayashi, M., and Hinuma, S. (2004) N-formylated humanin activates both formyl peptide receptor-like 1 and 2. *Biochem. Biophys. Res. Commun. 324*, 255–261.
6. Hashimoto, Y., Suzuki, H., Aiso, S., Niikura, T., Nishimoto, I., and Matsuoka, M. (2005) Involvement of tyrosine kinases and STAT3 in humanin-mediated neuroprotection. *Life Sci. 77*, 3092–3104.
7. Zou, P., Ding, Y., Sha, Y., Hu, B., and Nie, S. (2003) Humanin peptides block calcium influx of rat hippocampal neurons by altering fibrinogenesis of Aβ1−40. *Peptides 24*, 679–685.
8. Ying, G., Iribarren, P., Zhou, Y., Gong, W., Zhang, N., Yu, Z.-X., Le, Y., Cui, Y., and Wang, J. M. (2004) Humanin, a newly identified neuroprotective factor, uses the G-protein-coupled formylpeptide receptor-like-1 as a functional receptor. *J. Immunol. 172*, 7078–7085.
9. Tashima, Y., Oe, R., Lee, S., Sugihara, G., Chambers, E. J., Takahashi, M., and Yamada, T. (2004) The effect of cholesterol and monosialoganglioside (GM1) on the release and aggregation of amyloid β-peptide from liposomes prepared from brain membrane-like lipids. *J. Biol. Chem. 279*, 17587–17595.
10. Torok, M., Milton, S., Kayed, R., Wu, P., McIntire, T., Glabe, C. G., and Langen, R. (2002) Structural and dynamic features od Alzheimer's Aβ peptide in amyloid fibrils studied by site-directed spin labeling. *J. Biol. Chem. 277*, 40810–40815.
11. Verdier, Y., and Penke, B. (2004) Binding sites of amyloid β-peptide in cell plasma membrane and implications for Alzheimer's disease. *Curr. Protein Pept. Sci. 5*, 19–31.
12. Yanagisawa, K., Odaka, A., Suzuki, N., and Ihara, Y. (1995) GM1 ganglioside-bound amyloid beta-protein (A beta): a possible form of preamyloid in Alzheimer's disease. *Nat. Med. 1*, 1062–1066.
13. Choo Smith, L.-P., Garzon-Rodriguez, W., Glabe, C. G., and Surewicz, W. K. (1997) Acceleration of amyloid fibril formation by specific binding of Aβ-(1−40) peptide to ganglioside-containing membrane vesicles. *J. Biol. Chem. 272*, 22987–22990.
14. Yip, C. M., and McLaurin, J. (2001) Amyloid-β peptide assembly: a critical step in- fibrillogenesis and membrane disruption. *Biophys. J. 80*, 1359–1371.
15. Burdick, D., Soreghan, B., Kwon, M., Kosmoski, J., Knauer, M., Henschen, A., Yates, J., Cotman, C., and Glabe, C. (1992) Assembly and aggregation properties of synthetic Alzheimer's A4/*b* amyloid peptide analogs. *J. Biol. Chem. 267*, 546–554.
16. Niikura, T., Chiba, T., Aiso, S., Matsuoka, M., and Nishimoto, I. (2004) Humanin. After the discovery. *Mol. Neurobiol. 30*, 327–340.
17. Niikura, T., Tajima, H., and Kita, Y. (2006) Neuronal cell death in Alzheimer's disease and a neuroprotective factor, humanin. *Curr. Neuropharmacol. 4*, 139–147.
18. Niikura, T., Hashimoto, Y., Tajima, H., Ishizaka, M., Yamagishi, Y., Kawasumi, M., Nawa, M., Terashita, K., Aiso, S., and Nishimoto, I. (2003) A tripartite motif protein TRIM11 binds and destabilizes Humanin, a neuroprotective peptide against Alzheimer's disease-relevant insults. *Eur. J. Neurosci. 17*, 1150–1158.
19. Guo, B., Zhai, D., Cabezas, E., Welsh, K., Nouraini, S., Satterthwait, A. C., and Reed, J. C. (2003) Humanin peptide suppresses apoptosis by interfering with Bax activation. *Nature 423*, 456–461.
20. Zhai, D., Luciano, F., Zhu, X., Guo, B., Satterthwait, A. C., and Reed, J. C. (2005) Humanin binds and nullifies Bid activity by blocking its activation of Bax and Bak. *J. Biol. Chem. 280*, 15815–15824.
21. Luciano, F., Zhai, D., Zhu, X., Bailly-Maitre, B., Ricci, J.-E., Satterthwait, A. C., and Reed, J. C. (2005) Cytoprotective peptide humanin binds and inhibits pro-apoptotic Bcl-2/Bax-family protein BimEL. *J. Biol. Chem. 280*, 15825–15835.

22. Arakawa, T., Niikura, T., Tajima, H., and Kita, Y. (2006) The secondary structure analysis of a potent Ser14Gly analog of antiAlzheimer peptide, humanin, by circular dicroism. *J. Pept. Sci. 12*, 639–642.
23. Arakawa, T., Kita, Y., and Niikura, T. (2008) A rescue factor for Alzheimer's diseases: discovery, activity, structure and mechanism. *Curr. Med. Chem. 15*, 2086–2098.
24. Arisaka, F., Niikura, T., Arakawa, T., and Kita, Y. (2008) The structure analysis of humanin analog, AGA(C8R)HNG17, by circular dichroism and sedimentation equilibrium: comparison with the parent molecule. *Int. J. Biol. Macromol. 43*, 88–93.
25. Benaki, D., Zikos, C., Evangelou, A., Livaniou, E., Vlassi, M., Mikros, E., and Pelecanou, M. (2005) Solution structure of humanin, a peptide against Alzheimer's disease-related neurotoxicity. *Biochem. Biophys. Res. Commun. 329*, 152–160.
26. Benaki, D., Zikos, C., Evangelou, A., Livaniou, E., Vlassi, M., Mikros, E., and Pelecanou, M. (2006) Solution structure of Ser14Gly-humanin, a potent rescue factor against neuronal cell death in Alzheimer's disease. *Biochem. Biophys. Res. Commun. 349*, 634–642.
27. Altenbach, C., and Hubbell, W. L. (1988) The aggregation state of spin-labeled mellitin in solution and bound to phospholipid membranes: evidence that membrane-bound mellitin is monomeric. *Proteins 3*, 230–242.
28. Langen, R., Isas, J. M., Luecke, H., Haigler, H. T., and Hubbell, W. L. (1998) Membrane-mediated assembly of annexin studied by site-directed spin labeling. *J. Biol. Chem. 273*, 22453–22457.
29. Bates, I. R., Boggs, J. M., Feix, J. B., and Harauz, G. (2003) Membrane-anchoring and charge effects in the interaction of myelin basic protein with lipid bilayers studied by site-directed spin labeling. *J. Biol. Chem. 278*, 29041–29047.
30. Pistolesi, S., Ferro, E., Santucci, A., Basosi, R., Trabalzini, L., and Pogni, R. (2006) Molecular motion of spin labeled side chains in the C-terminal domain of RGL2 protein: a SDSL-EPR and MD study. *Biophys. Chem. 123*, 49–57.
31. Mchaourab, H. S., Hyde, J. S., and Feix, J. B. (1993) Aggregation state of spin-labeled cecropin AD in solution. *Biochemistry 32*, 11895–11902.
32. Mchaourab, H. S., Hyde, J. S., and Feix, J. B. (1994) Binding and state of aggregation of spin-labeled cecropin AD in phospholipid bilayers: effects of surface charge and fatty acyl chain length. *Biochemistry 33*, 6691–6699.
33. Bhargava, K., and Feix, J. B. (2004) Membrane binding, structure, and localization of cecropin-mellitin hybrid peptides: a site-directed spin-labeling study. *Biophys. J. 86*, 329–336.
34. Pistolesi, S., Pogni, R., and Feix, J. B. (2007) Membrane insertion and bilayer perturbation by antimicrobial peptide CM15. *Biophys. J. 93*, 1651–1660.
35. Der-Sarkissian, A., Jao, C. C., Chen, J., and Langen, R. (2003) Structural organization of alpha-synuclein fibrils studied by site-directed spin labeling. *J. Biol. Chem. 278*, 37530–37535.
36. Jayasinghe, S. A., and Langen, R. (2004) Identifying structural features of fibrillar islet amyloid polypeptide using site-directed spin labeling. *J. Biol. Chem. 279*, 48420–48425.
37. Margittai, M., and Langen, R. (2006) Spin labeling analysis of amyloids and other protein aggregates. *Methods Enzymol. 413*, 122–139.
38. Chen, M., Margittai, M., Chen, J., and Langen, R. (2007) Investigation of alpha-synuclein fibril structure by site-directed spin labeling. *J. Biol. Chem. 282*, 24970–24979.
39. Stewart, J. C. (1980) Colorimetric determination of phospholipids with ammonium ferrothiocyanate. *Anal. Biochem. 100*, 10–14.
40. Choi, J., Zhai, D., Zhou, X., Satterthwait, A., Reed, J. C., and Marassi, F. M. (2007) Mapping the specific cytoprotective interaction of humanin with the pro-apoptotic protein Bid. *Chem. Biol. Drug Des. 70*, 383–392.
41. Han, X., Holtzman, D. M., and McKeel, D. W.Jr. (2001) Plasmalogen deficiency in early Alzheimer's disease subjects and in animal models: molecular characterization using electrospray ionization mass spectrometry. *J. Neurochem. 77*, 1168–1180.
42. Waschuk, S. A., Elton, E. A., Darabi, A. A., Fraser, P. E., and McLaurin, J. (2001) Cellular membrane composition defines A lipid interactions. *J. Biol. Chem. 276*, 33561–33568.
43. Yip, C. M., Elton, E. A., Darabie, A. A., Morrison, M. R., and McLaurin, J. (2001) Cholesterol, a modulator of membrane-associated Aβ-fibrillogenesis. *J. Mol. Biol. 311*, 723–734.
44. Ji, S.-R., Wu, Y., and Sui, S.-F. (2002) Cholesterol is an important factor affecting the membrane insertion of a β-amyloid peptide (Aβ1−40), which may potentially inhibit the fibril formation. *J. Biol. Chem. 277*, 6273–6279.
45. Ramakrishnan, M., Jensen, P. H., and Marsh, D. (2003) α-Synuclein association with phosphatidylglycerol probed by lipid spin labels. *Biochemistry 42*, 12919–12926.
46. Ramakrishnan, M., Jensen, P. H., and Marsh, D. (2006) Association of α-synuclein and mutants with lipid membranes: spin-label ESR and polarized IR. *Biochemistry 45*, 3386–3395.
47. D'Errico, G., D'Ursi, A. M., and Marsh, D. (2008) Interaction of a peptide derived from glycoprotein gp36 of feline immunodeficiency virus and its lipoylated analogue with phospholipid membranes. *Biochemistry 47*, 5317–5327.